American Journal of Pathology, Vol. 166, No. 6, June 2005

Gastrointestinal, Hepatobiliary and Pancreatic Pathology

The Roles of Leptin and Adiponectin

A Novel Paradigm in Adipocytokine Regulation of Liver Fibrosis and Stellate Cell Biology

Xiaokun Ding,* Neeraj K. Saxena,* Songbai Lin,* Amin Xu,† Shanthi Srinivasan,* and Frank A. Anania*

From the Department of Medicine, Division of Digestive Diseases, Emory University School of Medicine, Atlanta, Georgia; and the Department of Medicine,† The University of Hong Kong, Hong Kong, China*

Although leptin is a key adipokine promoting liver fibrosis, adiponectin may prevent liver injury. To determine the role of these adipokines in liver fibrosis and to understand their expression *in vivo*, *fa/fa* rats and their lean littermates were subjected to bile duct ligation (BDL). Histomorphometry for collagen and α-smooth muscle actin (α-SMA) revealed that lean rats, but not *fa/fa* littermates, had significant fibrosis with abundant hepatic stellate cell (HSC) activation. The lean-BDL rats had significantly higher leptin concentrations in the hepatic vein than lean sham-operated, *fa/fa* BDL, or *fa/fa* sham-operated rats. Co-localization of leptin and α-SMA in activated HSCs was observed by immunohistochemistry. Real-time reverse transcriptase-polymerase chain reaction and Western blot analysis confirmed the presence of leptin and α-SMA in activated, but not quiescent, HSCs, whereas only quiescent HSCs synthesized adiponectin mRNA and protein. Adiponectin overexpression in activated HSCs reduced proliferation, augmented apoptosis, and reduced expression of α-SMA and proliferating cell nuclear antigen. Adiponectin receptors (AdipoR1 and AdipoR2) were detected in both activated and quiescent HSCs, but only activated HSCs produced significant apoptosis after treatment with either globular or full-length adiponectin. Adiponectin may act to reverse HSC activation, maintain HSC quiescence, or significantly, may have important therapeutic implications in liver fibrosis. *(Am J Pathol 2005, 166:1655–1669)*

Leptin, a 16-kd hormone, has an array of biological effects. Recently, leptin has been shown by several groups to be critical in the development of hepatic fibrosis;[1–4] however, in all of the previous work, hepatotoxic chemicals, such as carbon tetrachloride (CCl_4) and thioacetamide, have been used to demonstrate that the absence of circulating leptin or appropriate leptin signal transduction prevents liver fibrosis. As has also been widely described, a hypothesis for the development of nonalcoholic fatty liver (NAFL), which can lead to nonalcoholic steatohepatitis (NASH) and cirrhosis, rests on the upregulation of cytochrome P450 2E1 (CYP2E1) and 4A (CYP4A).[5,6] *In vivo* rodent models using hepatotoxins introduce confounding variables because their actions result in increased CYP2E1 activity,[7] which could be responsible for enhanced leptin production. It is also unclear whether leptin production is increased in injured liver, and if so by which liver cell population. Hepatic leptin production would be novel because leptin synthesis occurs primarily in omental fat and other adipose tissue.[8] We, and others, have demonstrated that leptin is present in activated stellate cells.[9,10]

In the present study, we used Zucker (hereafter *fa/fa*) rats and their lean littermates to determine whether an impaired leptin signal transduction system would fail to result in liver fibrosis in the bile duct liver injury model.[11] The *fa/fa* rat represents a recessive obesity mutation[12,13] rendering the animal diabetic and obese. The full expression of the *fatty* mutation is recessive, or *fa/fa*. The *fa*

Supported by the United States Public Health Service (grants AA 12933 and DK 062092 to F.A.A.) and the Department of Medicine, Emory University School of Medicine (to F.A.A.), and DK067045 (to S.S.); R24 DK064399; also, Emory Digestive Disease Center.

X.D. and N.K.S. contributed equally to the article.

Accepted for publication February 28, 2005.

Address reprint requests to Frank A. Anania, M.D., F.A.C.P., Room 248, Whitehead Biomedical Research Building, Division of Digestive Diseases, Department of Medicine, Emory University School of Medicine, 615 Michael St., Atlanta, GA 30322. E-mail: fanania@emory.edu.

mutation results in a missense mutation in the extracellular domain of the leptin receptor (OB-R), which results in a glutamine[269] to proline[269] amino acid substitution.[14,15]

At present there is not a clear hypothesis linking nonalcoholic fatty liver disease (NAFLD) and liver fibrosis. Reports indicate that circulating free leptin levels are significantly higher in NASH patients.[16,17] The pathogenic relationship among obesity, the metabolic syndrome, and NAFLD bears careful scrutiny and molecular mechanisms to understand the role of adipokines—hormones normally secreted by white adipose tissue—may not only play a role in the metabolic complications of obesity, but may also be a critical link in our understanding of the relationship between the clinical conditions associated with metabolic syndrome, NAFLD, NASH, and cirrhosis.[18,19]

A recent report demonstrated that adiponectin is protective against liver injury from alcoholic and nonalcoholic fatty liver in part from a resultant increase in carnitine palmitoyltransferase I and fatty acid oxidation.[20] A second report revealed increased sensitivity to carbon tetrachloride-induced liver fibrosis in adiponectin knockout mice, which was prevented when injection of adenovirus-producing adiponectin was given before carbon-tetrachloride.[21] Adiponectin is a relatively abundant 30-kd plasma protein that until the present was felt to be secreted specifically from adipose tissue. The protein circulates in multimeric complexes at relatively high levels in healthy humans.[22] In general, adiponectin levels correlate negatively with percent body fat, and fasting plasma insulin.[23] Adiponectin exists in the circulation as a full-length protein (fAd) as well as a putative proteolytic cleavage fragment consisting of the globular C-terminal domain (gAd), which may have enhanced potency.[23,24]

Two receptor forms have been cloned for adiponectin that have unique distributions and affinities for the molecular forms of the protein.[25] AdipoR1 is a high-affinity receptor for gAd with very low affinity for fAd and AdipoR2 has intermediate affinity for both forms of adiponectin.[25] AdipoR1 is abundantly expressed in skeletal muscle,[26] whereas, AdipoR2 is predominantly expressed in whole liver. These findings are consistent with the observation that fAd has a greater effect on hepatic metabolic signaling.[27]

The present study, therefore, provides novel physiological data linking metabolic syndrome, of which NAFLD and NASH are accepted components,[28] to cirrhosis. We also demonstrate, for the first time, that adiponectin, an adipokine thought to be exclusively secreted by adipocytes,[29] may be critical to either maintaining the hepatic stellate cell (HSC) quiescent phenotype or reverse hepatic fibrosis by induction of activated HSC apoptosis. Taken together, our data provide one mechanism to account for the recent data *in vivo* demonstrating the exquisite sensitivity to carbon tetrachloride by adiponectin knockout mice.[22] We also demonstrate that AdipoR1 and AdipoR2 are detected in both quiescent and activated HSCs by mRNA and protein and that activated HSCs have the potential to respond to both adiponectin isoforms because we demonstrate that fundamental biological properties of the activated HSC can be altered by adiponectin exposure.

Materials and Methods

Materials

Super Frost Plus slides, hematoxylin stain, and mounting media are from Fisher Scientific (Pittsburgh, PA). Anti-smooth muscle α-actin antibodies (Oncogene Research Products, San Diego, CA); anti-leptin antibodies (R&D Systems, Minneapolis, MN); anti-proliferating cell nuclear antigen (PCNA), anti-β-actin (Sigma Chemical Co., St. Louis, MO); anti-adiponectin antibody (a gift from Dr. Aimin Xu, University of Hong Kong, Hong Kong, China); anti-FLAG (Sigma); normal donkey serum, biotin-SP-conjugated AffiniPure donkey anti-rabbit IgG, biotin-SP-conjugated AffiniPure donkey anti-mouse IgG, peroxidase-conjugated streptavidin (Jackson ImmunoResearch Laboratories Inc., West Grove, PA); TSA Reagent Plus Cyanine3 system, TSA Reagent Plus FITCH system (Perkin Elmer Life Sciences, Boston MA); avidin-biotin blocking kit, Elite kit, biotinylated anti-mouse or anti-rabbit IgG (H+L), Nova Red substrate (Vector Laboratories, Burlingame, CA). Diaminobenzidine tetrahydrochloride, nickel sulfate hexahydrate, sodium acetate, hydrogen peroxide (30%), methanol, paraformaldehyde, and Sirius Red stain (Sigma). Rat leptin endocrine immunoassay was purchased as a service from Linco Research, St. Charles, MO. Dulbecco's modified Eagle's medium, trypsin-ethylenediamine tetraacetic acid, penicillin-streptomycin were all purchased from Invitrogen (Carlsbad, CA). Fetal bovine serum (FBS) was purchased from (HyClone, Logan, UT). Antibodies to caspase 3, cleaved caspase 3, and mitogen-activated protein kinase (MAPK) were all purchased from Cell Signaling (Beverly, MA); antibodies to adiponectin receptors 1 (AdipoR1) and 2 (AdipoR2) were purchased from Alpha Diagnostic (San Antonio, TX). Globular adiponectin (gAd) was purchased from Peprotech (Rocky Hill, NJ); full-length adiponectin (fAd) was purchased from Biovender (Candler, NC). Matrigel was purchased from BD Biosciences (Bedford, MA).

Animal Model for in Vivo *Studies*

Four-week-old *fa/fa* rats and their lean littermates were purchased from Charles River Laboratories (Wilmington, MA). Animals were housed for 4 additional weeks in a temperature-controlled environment (20 to 22°C) with a 12:12 hour light:dark cycle, and fed *ad libitum* with Purina Laboratory Chow (Ralston Purina, St. Louis, MO) and water. The bile duct ligation (BDL) protocol was approved by the Institutional Animal Care and Use Committee of Emory University. Rats were assigned to one of four groups ($n = 10$): BDL (lean, or LLB), BDL (*fa/fa*, or FFB) ($n = 10$), sham-operated (lean, LLN), and sham-operated (*fa/fa*, or FFN). BDL or sham operation was performed as described elsewhere.[30]

Twenty-one days after surgery, we anesthetized rats, established intravenous access via the right atrium, and also established portal venous access with a 16-gauge intravenous catheter. To calculate concentration of leptin for each rat, 1 ml of whole blood was collected from the portal vein and 1 ml hepatic vein blood was collected

from the right atrium after ligation of the vena cava. Total hepatectomy was performed and the animal was exsanguinated. Livers harvested were weighed and a portion was either snap-frozen in liquid nitrogen or placed in formalin fixative and paraffin-embedded for staining and immunohistochemical analysis. Serum from whole blood was used to measure alkaline phosphatase, total bilirubin, alanine aminotransferase, and aspartate aminotransferase. Serum chemistry was performed with a serial multichannel analyzer in the Department of Veterinary Resources at Emory University.

Leptin and Adiponectin Immunoassay

Plasma was collected using ethylenediamine tetraacetic acid as an anticoagulant. Controls, supplied by the manufacturer, were run simultaneously with samples. All assays were run three times in duplicate with standards from Linco Research (St. Charles, MO). The manufacturer also assisted in these determinations.

Picrosirius Red Staining and Immunohistochemical Staining for α-Smooth Muscle Actin (α-SMA)

Picrosirius red staining was used to detect collagen fibrils as described elsewhere.[31] Paraffin-embedded tissues were sectioned at 6 μm. Deparaffinized sections were placed in 95% ethanol and rinsed thoroughly in double-distilled water. Primary incubation with anti-α-SMA (1:800) was performed for 36 to 48 hours at 4°C in a closed humidity chamber.

Slides were viewed with a Nikon E1000M microscope (Melville, NY), and photographed with a Cool Snap color digital camera (Roper Scientific GmbH, Germany). Quantitative analysis of collagen in Picrosirius-stained or α-SMA-stained liver sections was performed by morphometric analysis. All images were quantified using ImagePro Plus version 4.5, a commercially available software package from Media Cybernetics (Silver Spring, MD). Imaging tissue sections was automated using an Image-Pro Plus macro calibrated for each microscope objective.

All sections were examined by the same person in which 10 random areas of interest were examined per liver section which was identified by computer-generated field identification. The operator who performed the collagen quantitation analyses was blinded to the identification of the individual slides examined. At least 15 different liver sections were examined for five individual animals for each treatment group. The tissue section on the slide was automatically scanned using a preselected threshold such that captured bright-field images were digitized into a series of picture elements (pixels). Areas of interest were selected from a specific section on each slide with the position of the tissue section recorded as counted from the slide label. Similar sections were then analyzed on each subsequent slide and the images saved for analysis. Background images were stored and subtracted from each capture area of interest. Data for both collagen and α-SMA were expressed as the mean percentage of total hepatic area in the tissue sections: the total area stained was divided by the total area of the slide (μm^2) and multiplied by 100 to give percentage of area stained. This calculation resulted in the determination of the percent area staining positively for collagen fibers providing a quantitative value on a continuous scale. Identical image analysis was performed on 6-μm sections in which staining with anti-α-SMA-antibody was used.

Immunohistochemistry to Detect Leptin with α-SMA-Positive Cells

Paraffin-embedded tissues were sectioned at 6 μm and deparaffinized. Deparaffinized sections were placed in 95% ethanol and rinsed thoroughly in double- distilled water. To detect leptin, slides were boiled in 10 mmol/L sodium citrate (pH 6.0) for 5 minutes and then allowed to cool for an additional 20 minutes. Three percent solution of H_2O_2 prepared in KPBS (potassium-phosphate buffered saline; Sigma) for slide incubation for 10 minutes was used for subsequent washes. Slides were incubated with avidin reagent for 15 minutes and subsequently washed, followed by incubation with biotin for 15 minutes, and washed again. Primary incubation with anti-α-SMA (1:800) was for 36 to 48 hours at 4°C in a closed humidity chamber.

Biotinylated secondary antibodies (1:600) were used for 1 hour at room temperature, and slides were incubated with either diaminobenzidine tetrahydrochloride (DAB) alone or nickel sulfate-DAB (NiDAB) for 20 minutes. Slides were monitored for color precipitate and anti-leptin (1:200) to stain tissues as described previously for anti-α-SMA. In place of DAB or NiDAB substrate, Nova Red substrate was used to detect leptin. Slides were subsequently counterstained in hematoxylin, decolorized in acid, and prepared for examination. Slides were viewed with a Nikon E1000M microscope, and photographed with a Cool Snap color digital camera (Roper Scientific). IPLab (Scanalytics, Fairfax, VA) was used for image analysis.

Real-Time Quantitative Reverse Transcriptase-Polymerase Chain Reactions (RT-qPCR) from Whole Liver after BDL to Detect Collagen, Leptin, and α-SMA

Total RNA from either whole liver or HSCs from BDL-injured rats was obtained using Trizol reagent (Invitrogen). The cDNA template was prepared using oligo-dT and random hexamer primers and Maloney murine leukemia virus reverse transcriptase as previously described in detail.[32] After the reverse transcription reaction, the cDNA template was amplified by polymerase chain reaction with *Taq* polymerase (Invitrogen). The following genes as listed in Table 1 were subjected to real-time RT-PCR analysis and their abundance was normalized against 18srRNA. All nucleotide sequences de-

Table 1. Genes Used in Real-Time RT-PCR Analysis

Accession no.	Gene	Sequence 5′ → 3′
NM013076	Leptin (F)	TTGTCACCAGGATCAATGACATTT
	Leptin (R)	GACAAACTCAGAATGGGGTGAAG
NM021578	TGF-β1 (F)	TGCCCTCTACAACCAACACA
	TGF-β1 (R)	GTTGGACAACTGCTCCACCT
X06801	α-SMA (F)	CCGAGATCTCACCGACTACC
	α-SMA (R)	TCCAGAGCGACATAGCACAG
XM213440	α1(1) collagen (F)	GAGTGAGGCCACGCATGA
	α1(1) collagen (R)	AGCCGGAGGTCCACAAAG
XM66209	α2(1) collagen (F)	TGATACCTCCGCTGGTGACC
	α2(1) collagen (R)	TAGGCACGACGTTACTGCAA
AY033885	Adiponectin (F)	AATCCTGCCCAGTCATGAAG
	Adiponectin (R)	TCTCCAGGAGTGCCATCTCT
BC061838	Adiponectin receptor 1 (F)	GGACTTGGCTTGAGTGGTGT
	Adiponectin receptor 1 (R)	AGGAATCCGAGCAGCATAAA
XM232323	Adiponectin receptor 2 (F)	GGCAGATAGGCTGGCTAATG
	Adiponectin receptor 2 (R)	CACCAGCAACCACAAAGATG

F, forward primer; R, reverse primer.

signed and outlined in Table 1 spanned two introns to prevent genomic DNA amplification.

For distinguishing the specific PCR product from nonspecific products and primer-dimers, melting curve analyses were used.[33,34] Because different DNA products melt at different temperatures, it was possible to distinguish genuine products from primer dimers or nonspecific products. Indeed, great care was taken to use PCR primers, which yielded a single product, an empirical process often requiring the design of several primer pairs. All PCR products were verified by sequencing dye termination technology; products were separated on 1% agarose gels, stained with ethidium bromide, and photographed using ultraviolet illumination. For quantification, we used real-time RT-PCR (LightCycler; Roche Molecular Biochemicals, Mannheim, Germany) using SYBR green as the fluorophore (Molecular Probes, Eugene, OR).

Isolation and Culture of Primary HSCs

Quiescent stellate cells were isolated as described in detail elsewhere.[35] Sprague-Dawley rats were purchased from (Charles River, Boston, MA). All rats received humane care, and the Institutional Animal Care and Use Committee of Emory University approved the HSC isolation protocol. In brief, *in situ* perfusion of the liver with 20 mg/dl of Pronase (Boehringer Mannheim, Indianapolis, IN) followed by collagenase (Cresecent Chemical, Hauppauge, NY), dispersed cell suspensions were layered on a discontinuous density gradient of 8.2% and 15.6% Accudenz (Accurate Chemical and Scientific, Westbury, NY). The resulting upper layer consisted of more than 95% HSCs. Cells were placed in modified medium 199 OR containing 20% FBS (Flow Laboratories, Naperville, IL). The purity of cells was assessed by immunolocalization of α-SMA in the monolayer as well as by intrinsic autofluorescence. The viability of all cells was verified by phase-contrast microscopy as well as the ability to exclude propidium iodide. Cell viability of cultures used for experiments was greater than 95%. Subconfluent activated cells in culture (75%) 7 to 10 days after isolation were washed twice with phosphate-buffered saline (PBS) and serum-starved for 16 hours with 0.1% FBS and 1% penicillin-streptomycin in Dulbecco's modified Eagle's medium.

Immunoblot Analysis for Leptin and Adiponectin in Quiescent and Activated Stellate Cells

Culture-activated HSCs and quiescent HSCs, harvested immediately after liver perfusion, were washed in PBS and resuspended in ice-cold RIPA buffer (10 μmol/L Tris-HCl, pH 8.0, 100 mmol/L NaCl, 1 mmol/L ethylenediamine tetraacetic acid, 1% Nonidet P-40, 0.5% sodium deoxycholate, 0.1% sodium dodecyl sulfate, and protease inhibitor cocktail, 10 μl/per ml; Sigma) for 30 minutes on ice. HSC lysates were centrifuged at 14,000 rpm for 30 minutes at 4°C. The supernatant was harvested and protein concentrations were determined using Bradford reagent (Sigma).[36] Proteins were resolved on 10% sodium dodecyl sulfate-polyacrylamide gel electrophoresis (50 μg/lane) and transblotted to nitrocellulose membranes.[37] Membranes were stained with Ponceau S (0.1%) to verify equal loading and transfer of proteins. After blocking with 1% bovine serum albumin in TBS-Tween 20 (20 mmol/L Tris-Cl (pH 7.5), 137 mmol/L NaCl, 0.05% Tween-20), membranes were incubated for 3 hours at room temperature with primary antibodies. Specific antibody binding was detected with corresponding horseradish peroxidase-conjugated secondary antibodies (1:5000) (Santa Cruz Biotechnology, Santa Cruz, CA). Equal protein loading was controlled by immunoblot of β-actin (dilution, 1:2000). To verify activation of HSCs with respect to quiescent phenotype, immunoblot for α-SMA (dilution, 1:2000) was also performed. To detect AdipoR1 and AdipoR2, immunoblot analysis was performed exactly as described above except that 100 μg/lane of protein was loaded on 12% sodium dodecyl sulfate-polyacrylamide gel electrophoresis and subsequently transferred as previously

described.[37] Immunoreactive proteins were revealed with the SuperSignal West Pico chemiluminescent substrate kit (Pierce, Rockford, IL) and then exposed to X-ray film (Kodak, Rochester, NY).

Transfection of HSCs with a Mammalian Expression Vector that Expresses FLAG-Tagged Full-Length Adiponectin (fAd)

The expression vector pcDNA-Ad-F, a kind gift from Dr. Aimin Xu (University of Hong Kong, Hong Kong, China), which encodes full-length adiponectin with a FLAG epitope tag at its C terminus was transfected into HSCs and COS-7 (used as a positive control for adiponectin production as described elsewhere[29]) using LipofectAMINE Plus (Invitrogen). Approximately 60% confluent HSCs were transfected with 4 μg of plasmid DNA. Cells were observed to secrete adiponectin into serum-free medium (SF) after 48 hours. Culture media were harvested from transfected cell cultures for co-immunoprecipitation. Culture media were incubated with 4 μl of anti-FLAG, and the mixture rotated at 4°C for 8 hours followed by addition of 20 μl (packed volume) of anti-FLAG-M_2-Agarose beads incubated at 4°C overnight. The beads were collected by centrifugation and washed twice with 1.5 ml of ice-cold RIPA buffer with a commercially available protease inhibitor cocktail. The identity of the protein was confirmed by immunoblot as described previously.

Quantification of DNA/Cell Proliferation by Bromodeoxyuridine (BrdU) Incorporation in Presence of Adiponectin and Expression of α-SMA and PCNA in Presence of Adiponectin by Immunoblot

BrdU incorporation analysis was performed using an enzyme-linked immunosorbent assay (BrdU Cell Proliferation Assay; Calbiochem, San Diego, CA). Approximately 5×10^2 HSCs were cultured in 96-well plates, and 0.1 μg/well of plasmid DNA (pcmAdF or pcDNA3.1 as vector control) was transfected for 3 hours. HSCs were allowed to grow in complete media (containing 10% FBS) for 24 hours. After 24 hours of growth, HSCs were subjected to serum starvation (SF media, 0.1% FBS), which served as a negative control for proliferation. Some HSCs were treated with serum (complete medium with 10% FBS) which served as positive control for proliferation. BrdU was added and was immunodetected using anti-BrdU antibody provided by the manufacturer. Resultant immune complexes were quantified by spectrophotometry (AD340, Beckman Coulter). The color intensity was standardized to the number of proliferating cells. Identical experiments were performed to obtain additional HSC lysates from 100-mm^3 plates for immunodetection of both PCNA and α-SMA.

Immunocytochemical Study to Measure the Extent of Adiponectin-Induced HSC Apoptosis

Culture-activated HSCs were grown at a density of 2×10^3, and transfected with 1.0 μg of pcmAdF or pcDNA3.1 or pEGFP-N1 (to assess transfection efficiency and viable HSCs for vector control). HSCs were grown for 48 hours in complete media followed by HSC fixation. Fixed HSCs were blocked with 10% normal donkey serum in Tris-buffered saline (TBS) with 0.2% Triton X-100 for 1 hour at 25°C. Slides were subsequently incubated with anti-FLAG (adiponectin is tagged with FLAG), a rabbit polyclonal antibody at 1:200 in 1% normal donkey serum in TBS with Tween (TBST), or anti-α-SMA (1:200 mouse monoclonal) overnight at 4°C. After secondary antibody treatment and incubation with streptavidin-horseradish peroxidase (1:500) for 1 hour at 25°C, the FLAG-tagged slides were incubated with Tyramide signal amplification (TSA)-Plus reagent tagged with Cyanine3 (red stain) system; and, α-SMA-tagged slides were incubated with TSA-Plus reagent tagged with fluorescein (green stain) as per the manufacturer's instructions for 15 minutes at 25°C. Finally, slides were stained with Hoechst (2.5 mg/ml) for 3 minutes at 25°C,[38] mounted, and examined under fluorescence microscopy. Cell viability or percent apoptosis was scored for all transfected cells using Hoechst and number of green fluorescent (GFP-positive) cells for vector control and red fluorescent (FLAG-positive) cells for pcmAdF. The transfection efficiency was calculated using data from 10 microfields per transfection sample and was found to be $18 \pm 1.2\%$ in three independent determinations. FLAG-positive HSCs were co-localized with apoptotic (Hoechst-positive) cells from 10 microfields to calculate the rate of apoptosis, as well as to visualize α-SMA-positive staining.

Maintenance of HSC Quiescence on Matrigel and Treatment of HSCs with Full-Length Adiponectin (fAd) and Globular Adiponectin (gAd)

Freshly isolated HSCs were first activated by culture on plastic for 2 days to 1 week and then were resuspended after trypsinization. Cell were recovered by centrifugation, washed twice in Dulbecco's modified Eagle's medium with 10% FBS, and plated on growth factor-reduced Matrigel (Becton Dickinson, Mountain View, CA) as described in detail elsewhere[39] at an initial density of 1×10^6/ml and maintained at 37°C. Quiescent HSCs, maintained on Matrigel, as well as culture-activated HSCs on plastic, were cultured for 3 days. Cells were growth-arrested by incubation for 16 hours in SF-Dulbecco's modified Eagle's medium. Serum-starved quiescent and activated HSCs were treated with recombinant fAd or gAd at 10 μg/ml for 48 hours.

Immunoblot Analysis for Caspase 3 and Cleaved Caspase 3 (p19)

HSCs were grown on Matrigel or plastic, serum-starved for 16 hours in serum-free (SF) media, followed by adiponectin or serum treatment as described above. HSCs from Matrigel were recovered by disrupting the cell monolayer with a rubber cell scraper followed by treatment with Dispase (10 mg/ml, Sigma for 15 minutes at 37°C. Recovered HSCs were resuspended in 100 μl of cell lysis buffer (Cell Signaling, Beverly, MA) containing a commercially available protease inhibitor cocktail (Sigma). An equal amount of HSC protein lysate from various treatments (100 μg/lane) was subjected to electrophoresis and transblotted as described previously. Immunoblot was performed using polyclonal antibodies against caspase 3 and cleaved caspase 3 (1:1000) and immunodetection was as described previously in the article.

Cell Viability Assay in Presence of Either gAd or fAd

Cell viability analysis was also performed by estimating reduction of XTT [2,3-bis(2-methoxy-4-nitro-5-sulfophenyl)-2H-tetrazolium-5-carboxyanilide], using commercially available reagents (Roche) and executed according to the manufacturer's instructions. Three-day-old HSCs grown on plastic as well as culture-activated primary HSCs (second generation from the time of isolation) were plated at either plastic or Matrigel—to maintain quiescence—at an initial density of 2×10^3 cells/well, serum-starved overnight, followed by treatment under SF-conditions alone, 10% FBS, gAd or fAd (10 μg/ml) in SF media for 48 hours. XTT labeling reagent was added to each culture well to attain a final concentration of 0.3 mg/ml. After 4 hours exposure at 37°C, absorbance was measured at 450 and 690 nm using a 96-well plate reader (PowerwaveX 340; Bio-Tek Instruments, Summit, NJ). Pilot experiments verified that the cell densities used in all experiments performed were within the linear range of the XTT assay. A standard curve was prepared using cell densities from 1×10^3 to 1×10^6, and the results were calculated with respect to the number of cells.

Statistical Analysis

Animal experiments were performed with 8 to 10 animals in each treatment and control group. All data are expressed as means ± SE. Real-time RT-PCR analysis of whole liver tissue was with three random samples for each liver from all treatment groups and performed in triplicate. Immunoblot and HSC real-time analysis was performed with separate samples in triplicate. Significance between groups was determined by Student's *t*-test, two-tailed, with appropriate posthoc analysis. In all comparisons, a *P* value less than 0.05 was used to indicate a significant difference.

Results

Biochemical Parameters Indicate Effective BDL in Both fa/fa and Wild-Type Animals

Regardless of phenotype (*fa/fa* or lean littermate) total alkaline phosphatase and serum bilirubin were significantly higher in both groups subjected to BDL, but not in animals undergoing sham operation. Mean ALP was 372 ± 85.8 IU/L for BDL-treated *fa/fa* rats, and 237 ± 55.8 IU/L in lean BDL animals. These values were not significantly different ($P = 0.06$). Mean serum total bilirubin for BDL-treated *fa/fa* rats was 4.4 ± 1.2 mg/dl; and for BDL-lean rats was 5.2 ± 1.2 mg/dl. These values were based on 10 different animals in each group subjected to BDL. By contrast, serum alanine aminotransferase levels were not affected by treatment, but were significantly different with respect to phenotype. Mean alanine aminotransferase values (ALT) in sham-operated *fa/fa* rats was 74.3 ± 14.4 U/L, and was 79.3 ± 11.4 U/L in BDL-treated *fa/fa* rats. In lean animals ALT values were as follows: sham-operated lean animals, 27.0 ± 9.5 U/L and in BDL-treated lean rats, 35.3 ± 6.8 U/L. The serum ALT values were not significantly different when comparisons were made between BDL and sham operations; rather, ALT values were statistically higher when comparing genotypic differences (*fa/fa* versus lean rats). These data are in keeping with what has been reported previously about the association between hepatic steatosis in *fa/fa* rats and serum ALT values.[40,41]

Lean Animals, but Not fa/fa Rats, Have Extensive Collagen Fibers and Bridging Fibrosis when Subjected to BDL

Figure 1 demonstrates Sirius red staining of representative liver sections after the 21-day BDL period. As expected, sham-operated controls had collagen fibers confined to either the portal triads or central veins (Figure 1, A and B; black arrows). Similar findings in BDL-operated *fa/fa* rats are shown in Figure 1C. In contrast, lean rats that underwent BDL have significant fibrosis (Figure 1D), including portal-portal bridging (Figure 1D, blue arrow) in transition to cirrhosis, with the development of nodules as displayed in this representative image. These data are representative of 10 animals per group in which five animals in each treatment group were examined in a single series of experiments for quantitative histomorphometry shown in the histogram in Figure 1E.

Immunohistochemistry from BDL-Operated Lean, but Not fa/fa Liver Sections, Reveals Significant α-SMA Staining

Figure 2, A, B, C, and E, reveal minimal α-SMA staining, which is, as expected, confined to supporting structures of the hepatic vasculature. Figure 2, at low power (Figure 2D) and at high power (Figure 2F), reveals an abundance of α-SMA in the liver lobules in a pattern similar to that

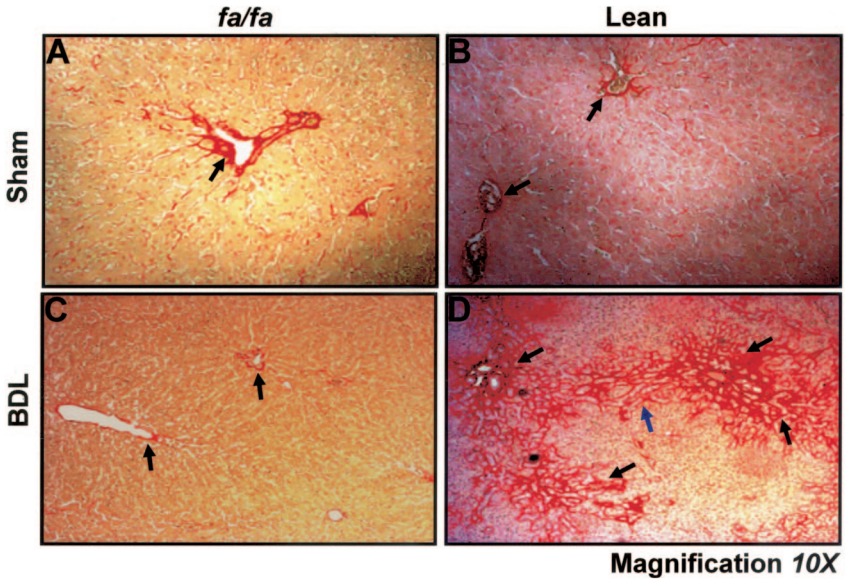

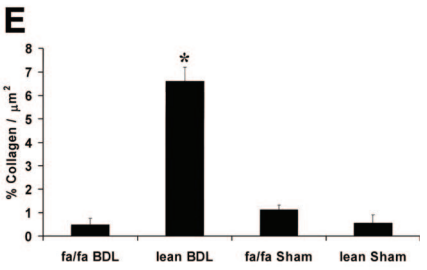

Figure 1. Picrosirius red stain for mature collagen reveals significant deposition in lean, but not *fa/fa*, rats subjected to BDL. Picrosirius red stain demonstrating collagen deposition principally found around supporting structures (**A–C**, **black arrows**). **D:** Representative image revealing collagen deposition (**black arrows**) as well as extensive bridging fibrosis (**blue arrow**) in transition to cirrhosis. **E:** Histogram representing image quantitation of the mean percent collagen fibers/total slide area scanned in $\mu m^2 \pm$ SEM determined as described in Materials and Methods. $^*P <$ 0.05, compares lean BDL versus sham-operated or *fa/fa* BDL rats. Original magnification, ×10 (**D**).

shown in Figure 1D where significant bridging fibrosis is present. Figure 2G is a representative histogram of quantitative histomorphometry performed for α-SMA immunostaining of liver sections from respective treatment groups which confirm a significant increase in α-SMA compared to all other treatment groups.

Leptin, but Not Adiponectin, Is Elevated in the Hepatic Vein of BDL-Operated Lean Rats

Figure 3 are the results of serum enzyme-linked immunosorbent assays taken from BDL-operated lean and *fa/fa* rats for mean leptin (Figure 3A) and adiponectin (Figure 3B) concentrations in the hepatic veins (HV) and portal veins (PV) of all examined animals before sacrifice. The data presented in Figure 3A indicate that the source of leptin in BDL-induced liver fibrosis is the injured liver. Mean circulating leptin concentrations were calculated to exclude artificially high concentrations of leptin from the portal venous circulation so as to determine whether or not the liver itself, when exposed to chronic injury, may produce leptin. Although it was anticipated that *fa/fa* rats, which have disrupted signal transducing ability, would also have high circulating leptin from peripheral adipose production, we failed to detect significantly higher leptin levels in the hepatic veins of BDL-operated *fa/*fa rats when compared to the mean concentration of leptin in the portal circulation. However, the mean leptin concentration measured from the hepatic veins of

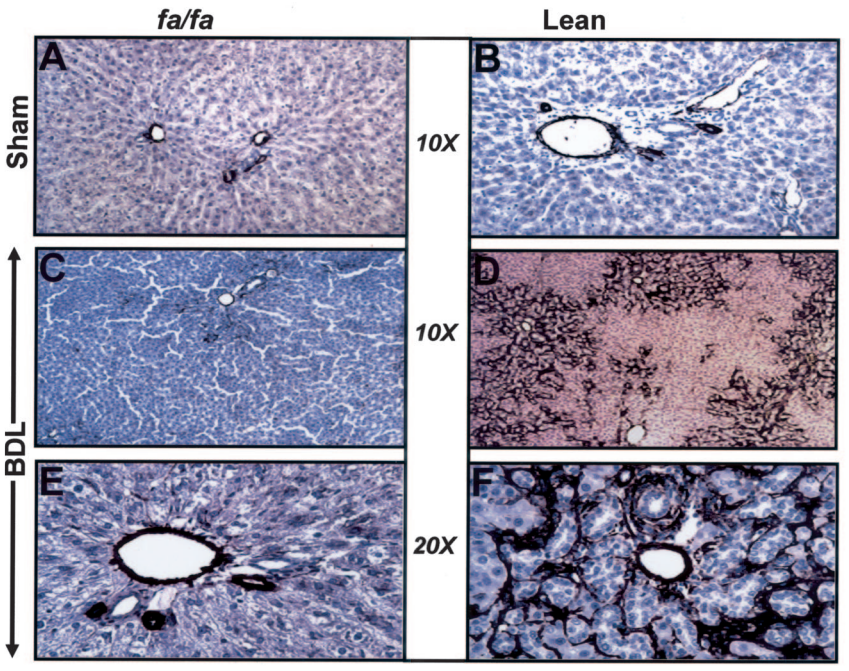

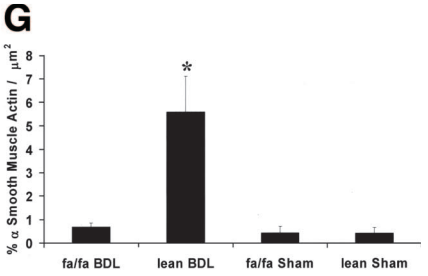

Figure 2. Low- and high-power magnification of immunohistochemical analysis for α-SMA in lean and *fa/fa* rats subjected to BDL. **A** and **B:** Representative photomicrographs of sham-operated *fa/fa* and lean littermates reveal α-SMA staining near supporting structures of vessels. **C** and **E:** Representative photomicrographs of BDL-operated *fa/fa* rats at low magnification (**C**) and high magnification (**E**) reveal similar staining pattern as in either *fa/fa* treatment group. **D** and **F:** Representative photomicrographs of immunohistochemical staining of BDL-operated lean animals. Low power (**D**) and high power (**F**) reveal significant lobular staining for α-SMA. **G:** Mean percent quantitation of α-SMA-positive cells/total slide area scanned in $\mu m^2 \pm$ SEM for respective animal groups, as described in Materials and Methods. $^*P < 0.05$, compares lean BDL versus sham-operated or *fa/fa* BDL animals. Original magnifications: ×10 (**A–D**); ×20 (**E**, **F**).

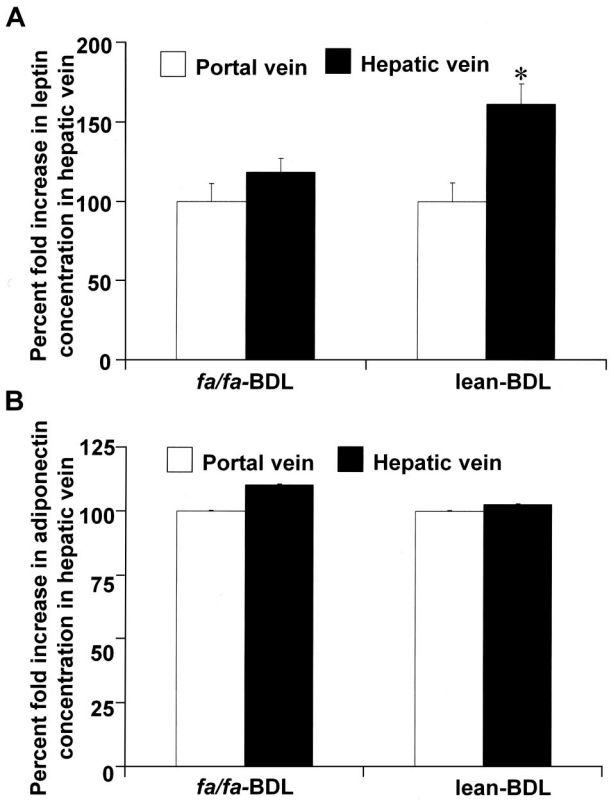

Figure 3. Percent increase of leptin but not adiponectin release in hepatic vein after BDL operations in *fa/fa* and their lean littermates. Leptin and adiponectin measurements were made by radioimmunoassay as described in Materials and Methods. Measurements were taken from both the portal (PV) and hepatic vein (HV) before sacrifice, and the mean differences were calculated to assess the mean circulating leptin and adiponectin concentration. Shown here is the percent fold increase of leptin and adiponectin concentrations in hepatic vein with respect to leptin or adiponectin levels in portal vein taken as 100%. Only lean littermates that underwent BDL showed a significant 1.5-fold increase of leptin levels in HV as compared to PV (*$P < 0.01$). This difference in leptin concentration from HV and PV was not observed in the *fa/fa* BDL group of rats. The same was true for adiponectin also and as shown in Figure 4B, no statistically significant difference of adiponectin was observed in HV and PV of lean BDL and *fa/fa* BDL group of rats ($P = 0.06$; $n = 10$ per treatment group, leptin concentrations in ng/ml). All of the rats from either the *fa/fa* or lean groups underwent sham operation without differences, in HV versus PV, for both leptin and adiponectin (data not shown here).

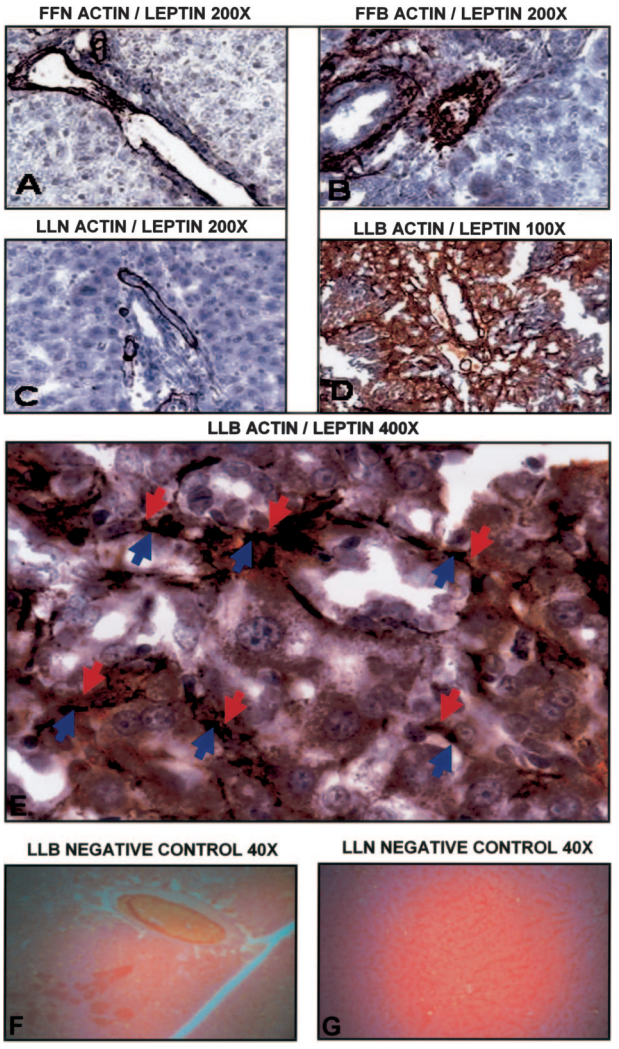

Figure 4. Immuno-co-localization of leptin and α-SMA by immunohistochemistry. Immuno-co-localization of leptin and α-SMA using double-labeling technique as described in Materials and Methods. α-SMA (labeled "actin" in photomicrographs) appears black (nickel diaminobenzidine substrate) and leptin appears brick red (Nova Red). Counter stain (azure blue) with hematoxylin. Figures with subtitles of experimental conditions as described with representative magnification: FFN, *fa/fa* sham-operated (**A**); FFB, *fa/fa* bile-duct ligated (**B**); LLN, lean sham-operated (**C**); LLB, lean bile-duct ligated (**D–E**). **E** demonstrates (**red arrows**, leptin; **blue arrows**, α-SMA) co-localization of leptin with α-SMA cells, corroborated in Figure 5 with real-time RT-PCR and Figure 3A, enzyme-linked immunosorbent assay for leptin (see text). **G** and **H:** Biotinylated secondary antibody without primary antibody from liver sections of LLB and LLN, respectively. Original magnifications, ×40 (**G**, **H**).

lean BDL operated rats was significantly higher when compared to the mean leptin concentration of the portal vein of the lean BDL cohort. Lean animals in the BDL group had a 1.5-fold increase in leptin in the hepatic vein when compared to portal vein concentrations (*$P < 0.05$). There was no significant difference in either circulating leptin or adiponectin concentrations in lean or *fa/fa* sham-operated animals (data not shown). There was also no significant difference in the hepatic vein adiponectin concentration in the lean BDL rats compared to the mean adiponectin concentration in the portal vein of these rats (Figure 3B). Although *fa/fa* BDL-operated adiponectin hepatic vein concentrations appeared to be increased over the portal vein, these data did not achieve statistical significance ($P = 0.06$, Figure 3B). These data suggest that the liver may be a significant source of leptin production in liver injury and these data are corroborated with Figures 4 and 5.

Leptin and α-SMA Co-Localize in the Lean Littermates of fa/fa Rats Subjected to BDL

Results of immunohistochemistry to determine whether leptin and α-SMA would co-localize to the same cells are shown in Figure 4. Alone, α-SMA stains black, and as can be seen in Figure 4, A, B, and C, is confined to supporting vascular structures. By contrast, leptin which stains red is absent in either sham-operated groups or in *fa/fa* BDL-operated rats. These photomicrographs are representative liver sections from sham-operated lean, *fa/fa* sham-operated, and *fa/fa* BDL-operated rats, respectively, indicating limited α-SMA

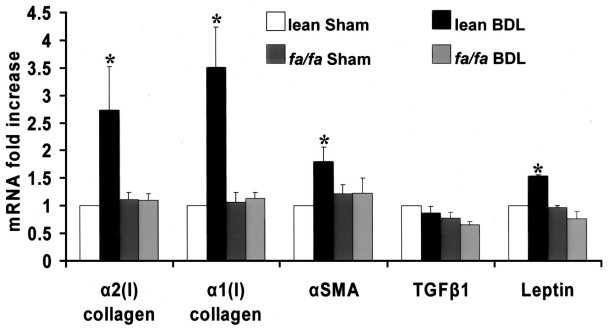

Figure 5. RT-qPCR analysis of α1(1) collagen, α2(1) collagen, α-SMA, TGF-β1, and leptin expression in whole livers from the four treatment groups. Expression of critical genes associated with liver fibrosis in each of the four treatment groups as outlined in the bar graph. Total RNA extracted from liver tissues was used to determine mRNA expression as described in Materials and Methods for α1(1) collagen, α2(1) collagen, α-SMA, TGF-β1, and leptin by real-time RT-PCR. Level of mRNA expression, observed in lean littermates sham-operated, was set as 100% of control. Results are means ± SE and represent 12 reactions for each treatment condition per gene analyzed. $^*P <$ 0.05 compared with lean sham-operated (control) values.

staining without leptin staining (indicated in red). Figure 4, D and E, includes representative photomicrographs from lean animals at low (×100, Figure 4D) and high power (×400, Figure 4E) magnification. In Figure 4E (×400) leptin staining and α-SMA staining appear to co-localize to the same cells, which is corroborated by RT-qPCR in Figure 5 and also supports data presented in Figure 2 that demonstrate abundant activated HSCs as a potential source for not only collagen production but increased leptin production as measured in the hepatic vein of BDL-operated lean rats. Figure 4, G and H, represents biotinylated secondary antibody, without primary antibody for either leptin or actin are controls at low power demonstrating lack of brick red or azure blue staining, respectively.

RT-qPCR Demonstrates Up-Regulation of Genes Associated with HSC Activation and Liver Fibrosis

Figure 5 represents RT-qPCR data for genes including α1(I) collagen, α2(I) collagen, α-SMA, transforming growth factor (TGF)-β1, and leptin from cDNA synthesized from whole liver RNA for each of the four treatment conditions previously described. Data were obtained from three samples for each of three whole livers for each of the four treatment conditions. RT-qPCR analysis of liver from lean BDL-operated animals indicated a 2.5-fold increase in α2(I) collagen gene expression, a 3.5-fold increase in α1(I) collagen gene expression, a 1.5-fold increase in α-SMA gene expression, and a 1.4-fold increase in leptin gene expression, with respect to lean sham-operated rats. All other treatment groups failed to have significantly increased expression of these molecules when compared to the lean sham-operated controls. Despite the importance of TGF-β1 in the development of liver fibrosis,[42] we could not detect a significant increase in TGF-β1 mRNA expression in the lean BDL-operated animals;

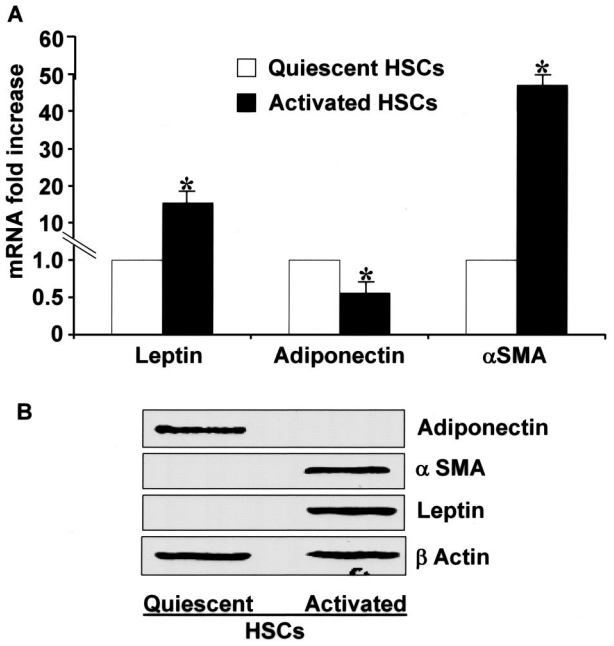

Figure 6. Adiponectin, α-SMA, and leptin mRNA expression and respective protein production reveal differential expression in quiescent and culture-activated HSCs. **A:** RT-qPCR was performed as described in the text. The level of mRNA expression observed in quiescent HSCs was set as control. Results are means ± SE and represent six reactions for both stellate cell phenotype and gene analyzed. $^*P <$ 0.05 compared with quiescent HSCs under corresponding conditions. **B:** Immunoblot analysis for adiponectin, α-SMA, and leptin in quiescent and activated HSCs. Freshly isolated quiescent and culture-activated HSCs were used to prepare lysate and were subjected to immunoblot for adiponectin, α-SMA, and leptin. β-Actin served as a loading control. These data are representative of multiple independent experiments.

and, TGF-β1 expression did not differ significantly among all four treatment groups.

Adiponectin and Leptin Expression and Expression Levels of Adiponectin Receptors in Quiescent and Culture-Activated HSCs Reveal Differential Patterns of Expression

We reasoned that if HSCs, as fat-storing cells, produced leptin on injury, or culture activation, then in quiescence, such cells would not only fail to do so but may produce adiponectin, which could promote, or maintain, HSC quiescence. In fact, as can be seen in Figure 6A adiponectin mRNA expression is markedly suppressed in HSCs from culture activation, but adiponectin is abundantly present in the quiescent phenotype. Even more striking is the absence of adiponectin in activated HSCs as assessed by immunoblot (Figure 6B). Figure 6A represents RT-qPCR analysis for leptin, adiponectin, and α-SMA expression in quiescent and culture-activated HSCs. Both leptin and α-SMA were increased 19-fold and 55-fold, respectively, in activated HSCs as compared to quiescent HSCs. On the other hand, the activated HSC phenotype resulted in significantly lower adiponectin mRNA than quiescent cells. Immunoblot studies revealed that leptin and α-SMA were present in activated, but not in quiescent HSCs as anticipated; whereas adiponectin appeared to be present only in quiescent HSCs (Figure 6B).

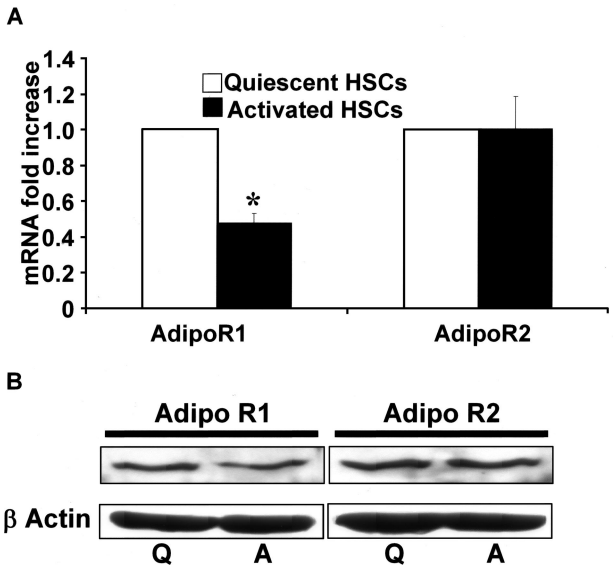

Figure 7. AdipoR1 and AdipoR2 are both expressed in quiescent and activated HSCs. **A:** RT-qPCR was performed as described in the Materials and Methods section. AdipoR2 did not display a differential level of expression when compared to quiescent cells by mRNA. **B:** Immunoblot analysis for AdipoR1 and AdipoR2 confirmed that protein for the respective isoforms were present in both quiescent (Q) and activated HSCs (A). All studies were performed three times in triplicate using separate HSC lysates. β-Actin served as a loading control.

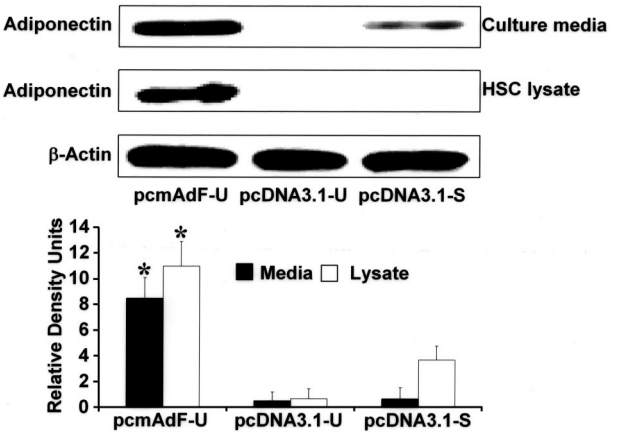

Figure 8. Transfection of the adiponectin expression vector (pcmAdF) results in HSC production of adiponectin. Control experiment demonstrating the consequence of adiponectin overexpression and respective controls with one of three vectors: pcmAdF (epitope encoding full-length adiponectin), pcDNA3.1-U (empty vector in SF conditions, 0.1%), and pcDNA3.1-S (empty vector in the presence of 10% FBS. The vectors and experimental conditions and nomenclature are also used in subsequent studies shown in Figure 9. Adiponectin expression in HSCs and culture media was assayed by immunoblot to assure HSC expression and secretion of adiponectin, which is shown in **lane 1**. In HSCs overexpressing pcDNA3.1-U in the absence of serum (**lane 2**) no adiponectin was detected in the cells nor the culture media, while very low adiponectin expression, after HSC transfection with pcDNA3.1 in the presence of 10% FBS (**lane 3**). Respective densitometry is shown for three independent experiments performed in triplicate; β-actin served as a loading control.

Hence, although activated HSCs synthesize leptin, interestingly, quiescent HSCs, but not activated ones, synthesize adiponectin.

Both the receptors for adiponectin, AdipoR1 and AdipoR2, were present in quiescent as well as culture-activated HSCs, however RT-qPCR revealed, mRNA expression of AR1 in activated HSCs was reduced by nearly 50% compared to quiescent HSCs (Figure 7A). The expression of AdipoR2 did not change (Figure 7A) in both HSC phenotypes. Immunoblot for both AdipoR1 and AdipoR2 demonstrated the presence of both receptor isoforms in both quiescent and activated HSCs (Figure 7B). These results are in keeping with the ability of HSCs to respond to both gAd and fAd.[25]

Adiponectin Results in Reduction of Culture-Activated HSC-BrdU Incorporation and PCNA Expression as Well as Reduction in α-SMA

To determine whether adiponectin could interfere with activated HSC viability, we first determined whether adiponectin expression in activated HSCs was adequate by transfection of pcmAdF, Figure 8 is a representative immunoblot indicating that both HSC lysate and secreted adiponectin resulted from the transfection of pcmAdF in SF media (pcmAdF-U). Neither transfection of the control vector in SF conditions (pcDNA3.1-U) nor the presence of the control vector with 10% FBS resulted in significant adiponectin production in HSC lysate or culture media. A small amount of adiponectin was present in the culture media when HSCs transfected with pcDNA3.1 was exposed to 10% FBS, however, this could be attributed to presence of some adiponectin in serum. The adiponectin present in HSC lysate under the same conditions, however, was absent.

Given effective adiponectin overexpression detected by pcmAdF transfection, we used the same experimental design to determine whether adiponectin expression would alter BrdU incorporation, the results of which are shown in Figure 9A. Overexpression of adiponectin in activated HSCs in SF conditions (pcmAdF-U) resulted in a significant decrease in HSC proliferation when compared to HSC transfection with vector control (pcDNA3.1-U) alone. Adiponectin overexpression markedly attenuated HSC proliferation to 10%, whereas the proliferation rate of HSCs transfected with vector control in the presence of 10% FBS (pcDNA3.1-S), was sevenfold higher (Figure 9A). PCNA, another marker of cell proliferation was significantly reduced by pcmAdF transfection of activated HSCs, as was the expression of α-SMA (Figure 9B); the later being an important marker of HSC activation. The absence of serum in transfected control HSCs did result in a reduction of both PCNA and α-SMA, but failed to achieve the marked reduction induced by adiponectin transfection.

Adiponectin Not Only Reduces the Expression of α-SMA, It Also Induces Apoptosis in HSCs as Assessed by Immunocytochemistry and Hoechst Staining

We also examined whether adiponectin overexpression would result in activated HSC apoptosis. Fluorescence microscopy of immunologically stained FLAG-tagged HSCs (transfected with pcmAdF for adiponectin) (Figure

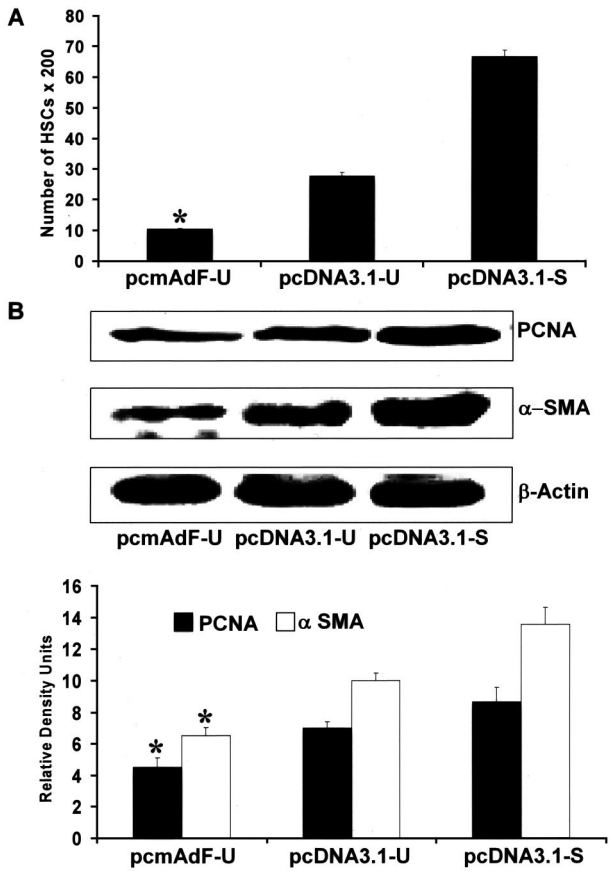

Figure 9. Adiponectin overexpression in activated HSCs markedly diminishes activated HSC proliferation and α-SMA content. **A:** The adiponectin expression vector, pcmAdF (epitope encoding full-length adiponectin), was transfected as described in Figure 8 and found to reduce activated HSC BrdU incorporation. HSCs were cultured in a 96-well plate, 0.1 μg per well of plasmid DNA was transfected: pcmAdF (epitope encoding full-length adiponectin), pcDNA3.1-U (empty vector under SF conditions), or pcDNA3.1-S (empty vector in the presence of 10% FBS). BrdU was added after 24 hours of transfection and HSCs were allowed to grow for another 48 hours in the presence or absence of serum. Incorporation of BrdU into newly synthesized DNA was immunodetected as described in Materials and Methods and intensity of color complex was assayed spectrophotometrically. Calorimetric results were standardized to number of cells and plotted here as mean ± SE of three independent experiments performed in triplicate. Adiponectin overexpression markedly attenuated HSC proliferation to 10%, whereas the proliferation rate of HSCs transfected with vector control in the presence of 10% FBS (pcDNA3.1-S), was significantly higher. $^{*}P < 0.01$, compared to untreated HSCs transfected with control vector (pcDNA3.1-U). **B:** Adiponectin vector transfection in SF-conditions (pcmAdF-U) in HSCs reduced protein expression levels of α-SMA and PCNA. To determine the effect of adiponectin on expression of α-SMA and PCNA, proliferation markers for HSCs, 4 μg of plasmid DNA, pcmAdF (epitope encoding full-length adiponectin), or pcDNA3.1 (vector control) were transfected into HSCs in 100-mm^3 plates. After 48 hours, HSC lysates were prepared, total protein was quantified and resolved by sodium dodecyl sulfate-polyacrylamide gel electrophoresis, followed by immunoblot analysis with antibodies against α-SMA and PCNA. β-Actin served as a loading control. Shown is a representative immunoblot for the same along with densitometric analysis of the results.

10A), when subject to Hoechst staining revealed that adiponectin overexpression resulted in apoptosis (Figure 10, B and C). These data were quantitated (Figure 10E) as percent HSC apoptosis divided by the total number of transfected HSCs from multiple microfields. A representative image (Figure 10D) demonstrates co-localization of α-SMA-positive and FLAG-tagged HSCs. The photomicrographs, from the same microfield, are representative of three independent experiments in which 10 microfields per experiment were used for quantitative determinations.

Adiponectin Also Induces Apoptosis of Activated HSCs but Fails to Do So in the Quiescent Phenotype and This Effect Is Mediated by Caspase 3

To determine whether or not adiponectin would induce quiescent HSC apoptosis, freshly isolated cells were grown and transferred to Matrigel to maintain quiescence as described in detail in Materials and Methods. Three-day-old activated HSCs or second generation (fully activated) HSCs, were grown on plastic chamber slides; all cell types were monitored for α-SMA to gauge respective states of activation. After serum starvation, cells were treated with either gAd or fAd as described. Hoescht staining (Figure 11A) of activated HSCs exposed to gAd or fAd revealed significantly increased apoptosis compared to quiescent HSCs grown on Matrigel. These results corroborate the findings illustrated in Figure 10 in which adiponectin was overexpressed in activated HSCs. Immunoblot analysis to probe for cleaved caspase 3 (p19) (Figure 11B) clearly demonstrated the presence of cleaved caspase 3 in gAd-treated activated HSCs; whereas cleaved enzyme was undetectable in either gAd-treated or fAd-treated quiescent cells. There was no effect of either gAd or fAd on MAPK phosphorylation in either HSC phenotype (data not shown). Finally, as shown in Figure 11C by XTT reduction, both gAd or fAd significantly reduced cell viability in activated HSCs (3 days and primary passaged second generation HSCs) but failed to do so in quiescent HSCs grown on Matrigel. These data corroborate that either gAd or fAd induced apoptosis in the activated HSC phenotype but not in quiescent cells. In fact, apoptosis or growth of the quiescent HSC was not affected by the presence of any treatment condition, including the presence of serum or serum starvation.

Discussion

Recent studies from several laboratories have demonstrated that leptin is a key adipokine in promoting liver fibrosis. In sharp contrast to most adipokines, adiponectin expression and serum concentrations are not increased,[43] but reduced in a variety of obese and insulin-resistant states including the metabolic syndrome which includes NAFLD. Like leptin, adiponectin has important physiological effects, including anti-atherogenic properties;[44] and, hypoadiponectinemia has been shown to be associated with coronary artery disease in humans.[45] Adiponectin may have anti-tumor effects by acting as a negative regulator of angiogenesis by inducing caspase-mediated endothelial cell apoptosis; this effect appears to be independent of AMP kinase-mediated signaling.[46] The present study provides clear physiological evidence for the role of the leptin-signaling axis in an *in vivo* model of cholestatic liver injury, and strengthens the hypothesis

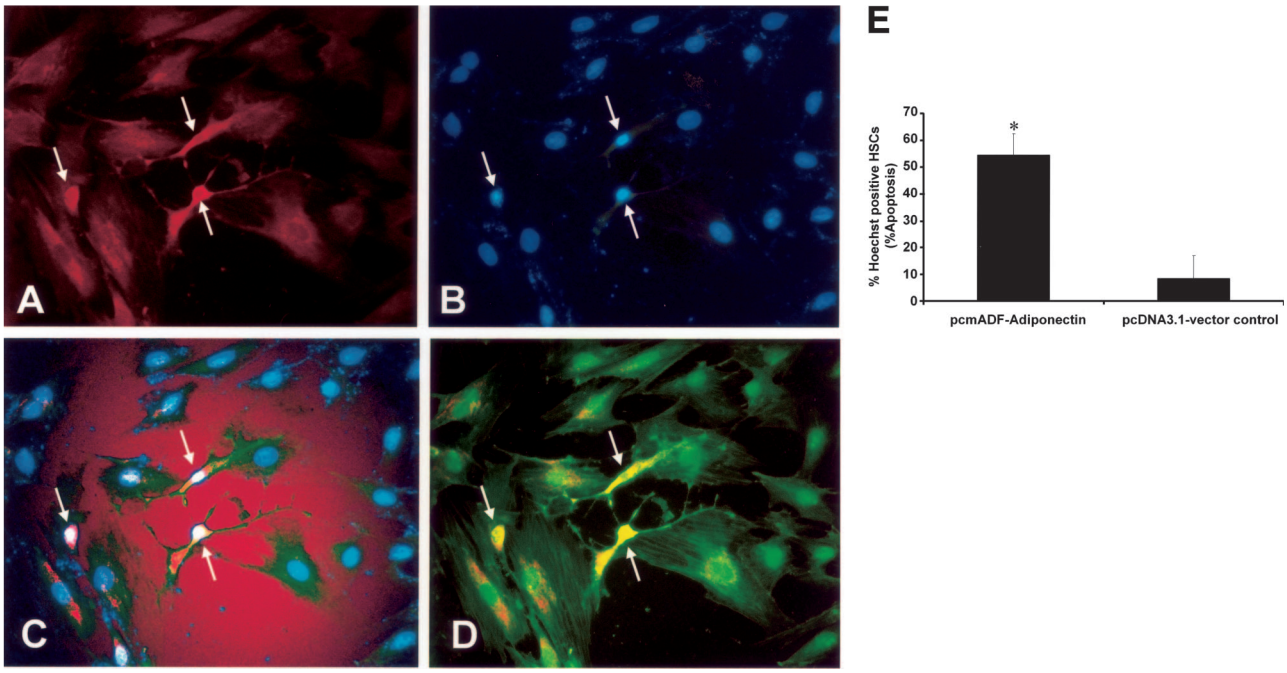

Figure 10. Adiponectin overexpression induces HSC apoptosis in α-SMA-positive cells. Culture-activated HSCs were grown onto chamber slides as described in the text, and transfected as described previously in Figures 8 and 9. pcmAdF, epitope encoding full length adiponectin; pcDNA3.1, vector control. **A:** HSCs were visualized by fluorescence microscopy to identify adiponectin and α-SMA-positive cells; apoptosis was analyzed by Hoechst staining.[38] **B:** Representative fluorescent photomicrograph of HSCs demonstrates presence of adiponectin-positive cells and the transfection efficiency for pcmAdF was 18 ± 1.2%; Hoechst staining demonstrates HSC apoptotic bodies. **C:** Co-localization of adiponectin-positive HSCs with Hoechst-positive HSCs. **D:** FLAG-tagged adiponectin-positive cells also co-localized with α-SMA-positive cells. All panels shown are from the same microfield and the same cells (**white arrows**). The percentage of apoptotic HSCs, shown in the bar graph was calculated as the number of apoptotic cells/the total number of FLAG-tagged adiponectin-positive cells and are compared to the number of apoptotic cells/HSCs successfully transfected with the vector control (9.4%) (*$P < 0.01$). The percentage of apoptotic HSCs represents the means ± SE of 10 high-power fields of three independent experiments performed in triplicate. Original magnification, ×400 (**A**).

that leptin is a key adipokine in promoting liver fibrosis. We also report, for the first time, that quiescent HSCs synthesize adiponectin; but adiponectin can induce activated HSC apoptosis by caspase activation and inhibit proliferation, failing to do so in quiescent HSCs. To our knowledge this is the first report of a potential mechanism whereby adiponectin is a potential anti-fibrotic therapy in chronic liver disease, particularly as it relates to nonalcoholic steatohepatitis.

As stated previously, a number of workers have shown that chemically induced acute and chronic liver injury, or the use of the methione-choline deficiency diet, require functioning leptin and leptin receptors for the development of liver fibrosis to ensue.[1–4] This study is the first to demonstrate, by using the bile-duct ligation injury model, in either Zucker (*fa/fa*) rats, or their lean littermates, that leptin and its signaling apparatus are an absolute requirement for extensive liver fibrosis and that such requirement is not an artifact of chemical injury in rodents. Both the *fa/fa* and lean animals subjected to BDL had significantly elevated serum total bilirubin and alkaline phosphatase, when compared to identical animals that underwent sham operation. Although both BDL-operated groups had significant cholestasis, only the lean animals developed significant fibrosis. Activation of HSCs results in the production of smooth muscle proteins in the cytoskeleton and is central to the development of hepatic fibrosis in chronic liver injury. Liver fibrosis, clearly demonstrated by Picrosirius red stain in Figure 1, is also substantiated by the presence of α-SMA (Figure 2). Activated HSCs are strikingly abundant in the BDL-treated lean littermates and beyond the portal structures where portal myofibroblasts are typically found.

The source of leptin that is responsible for ongoing liver injury is subject to dispute. We, and others, have already demonstrated that leptin mRNA and protein is present in activated, but not quiescent HSCs *in vitro*, and did not detect leptin production in Kupffer cells and hepatocytes.[9] These data are important because depot-related leptin expression varies in humans and is greater in subcutaneous adipocytes than in omental adipocytes;[47] however, because rat omental adipocyte expression may be altered,[48] we attempted to eliminate this potential source of leptin that may have been increased by BDL by measuring serum leptin concentrations in both the portal vein and the hepatic vein of all treated animals. Although we cannot entirely exclude that hepatic cells other than activated HSCs are responsible for this increase our data in Figure 3 reveal, at high magnification, that leptin co-localizes with α-SMA-positive cells. These microscopic findings were not present in any other treatment condition. We also cannot discount that leptin production from extrahepatic sources might be contributing to liver fibrosis, particularly in NASH; or that leptin release from hepatic stores may play a role because leptin bound to OB-Re, a circulating leptin-binding protein could potentially release free leptin in the liver,[49] our data convincingly show that a significant component of leptin in

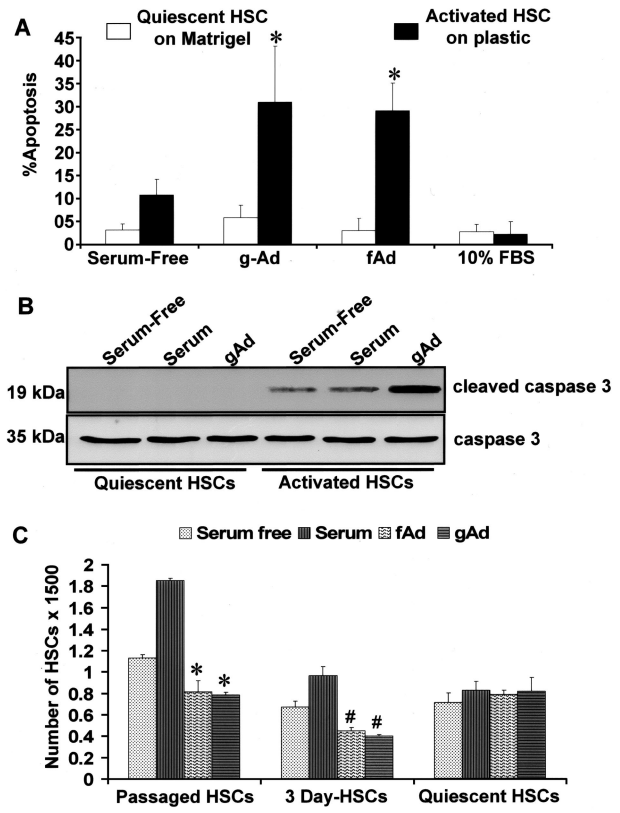

Figure 11. Adiponectin fails to induce apoptosis in quiescent HSCs but does in activated HSCs. **A:** After isolation of HSCs, cells were grown on Matrigel to maintain quiescence or on plastic as described in Materials and Methods. HSCs, exposed to gAd or fAd were analyzed for apoptosis by Hoechst staining. Both gAd and fAd significantly induced apoptosis in activated HSCs ($^*P < 0.01$). **B:** To determine whether or not caspase 3 played a role in activated HSC apoptosis, immunoblot analysis, shown here, revealed that adiponectin-treated activated HSCs resulted in increased cleaved caspase 3 (p19), which was not detected from quiescent HSC lysates. This experiment was performed with three different lysates. **C:** XTT analysis of HSC viability in the face of either gAd or fAd indicates that neither gAd or fAd or serum altered the viability of quiescent HSCs grown on Matrigel as described in detail in the text. In response to either form of adiponectin, however, either the 3-day-old primary cells or second generation passaged HSCs a marked reduction in cell viability was exhibited ($^*P < 0.01$, when compared to respective HSCs grown in the presence of 10% FBS; $^\#P < 0.05$, 3-day-old HSCs compared to respective cells grown in 10% FBS). The results are representative of multiple independent experiments.

liver injury arises from activation of HSCs; and that activated HSCs are a major source of leptin in the development of liver fibrosis. Although the absolute increase in leptin in the lean BDL-operated animals appears nominal, to our knowledge this is the first report of quantitative measurements related to an *in vivo* experiment, and future studies will need to be performed to define leptin concentrations that are physiologically necessary for profibrogenic actions. We also did not detect that leptin enhanced mRNA for TGF-β1 by RT-qPCR (Figure 5) in our *ex vivo* analysis for key genes associated with enhanced extracellular liver matrix. One explanation for this finding may be due to the fact that leptin is necessary for induction of bioactive TGF-β1 protein, however, and not nascent mRNA expression.[3] An alternative explanation may be that leptin increases TGF-β type II receptor expression as was previously demonstrated in mesangial cells from *db/db* mice.[50] Although the data presented suggest that leptin has the potential to act independent of TGF-β1, additional experiments to elucidate signal crosstalk between leptin and TGF-β1 may provide a more definitive explanation.

Leptin is one of six adipocytokines, including adiponectin that are thought to play a dynamic role in the development and maintenance of insulin resistance.[51] Because insulin resistance is central to the development of NASH, and as yet no direct link for insulin resistance has been established in development of liver fibrosis, we examined whether or not adiponectin expression was altered in HSCs either *ex vivo* or with the culture-activated *in vitro* model. Our rationale was based on two recently published reports[20,21] that indicate that adiponectin *in vivo* may be protective in liver injury because carbon-tetrachloride-induced liver fibrosis in adiponectin knockout mice was increased.[21]

The discrepancy between the absence of adiponectin protein and extremely low adiponectin mRNA expression in HSCs may be due to posttranscriptional or posttranslational modification involved in the synthesis and packaging of secreted adiponectin, and are consistent with a recent report concerning the expression of adiponectin.[52] Since this is the first report of HSC production of adiponectin, and our understanding of the regulation of adiponectin is rapidly developing, control of adiponectin gene regulation and synthesis in HSCs will need to be addressed in the near future.

Because adiponectin functions as a secreted protein, we further examined whether the presence of adiponectin receptors in HSCs existed. AdipoR2 is primarily found in liver whereas AdipoR1 has been reported to be found primarily in skeletal muscle. AdipoR1 as well as AdipoR2 were found to be present in both quiescent and culture-activated HSCs; however mRNA expression of AdipoR1 was reduced by 50% in activated HSCs as compared to quiescent HSCs (Figure 7A). Immunoblot confirmed the presence of both receptors in both quiescent and activated HSCs (Figure 7B). This would be consistent with the fact that we obtained similar results when activated HSCs were exposed to either gAd or fAd. Importantly, such treatment failed to induce quiescent HSC apoptosis or inhibit mitogenesis; whereas gAd or fAd had profound effects on activated HSCs, inhibiting mitosis and inducing caspase-mediated apoptosis. These data compliment the data obtained by overexpression of fAd in HSCs (Figure 10) and strongly support the proapoptotic action of adiponectin in activated, but not quiescent, HSCs (Figure 11). To our knowledge, this is the first report identifying both protein receptor isoforms in isolated HSCs. Expression of AdipoR1 and AdipoR2 serve as receptors for globular and full-length adiponectin, respectively, and traditionally are thought to mediate effect by enhanced AMP kinase activity,[53,54] PPAR-α ligand activities[55] as well as fatty-acid oxidation, and glucose uptake by adiponectin.[25]

Although additional molecular details need to be examined, this is the first report, providing a direct link between NASH, insulin resistance, and the metabolic syndrome on the one hand and liver fibrosis on the other. We have demonstrated by examining key cellular mech-

anisms—proliferation and apoptosis—a potential therapeutic mechanism whereby leptin, known to be associated with fibrosis, has an adipokine counterpart, adiponectin, that protects against liver fibrosis by induction of caspase-mediated apoptosis of activated HSCs. Hence adiponectin may have a positive and direct effect in the resolution of liver fibrosis. At this time we cannot determine which receptor isoform is more susceptible to adiponectin. Nonetheless, our findings provide a novel cellular and molecular explanation for the *in vivo* work published previously, demonstrating that adiponectin is protective against liver injury in NASH and is anti-fibrotic.[21,22] Importantly, this work lends data to confirm that one biological property of leptin is to enhance liver fibrosis, while establishing that adiponectin may have a novel and opposite effect.

Acknowledgment

We thank Ms. Donna Suresch for her excellent tissue preparation and analysis.

References

1. Honda H, Ikejima K, Hirose M, Yoshikawa M, Lang T, Enomoto N, Kitamura T, Takei Y, Sato N: Leptin is required for fibrogenic responses induced by thioacetamide in the murine liver. Hepatology 2002, 36:12–21
2. Leclercq IA, Farrell GC, Schriemer R, Robertson GR: Leptin is essential for the hepatic fibrogenic response to chronic liver injury. J Hepatol 2002, 37:206–213
3. Saxena NK, Ikeda K, Rockey DC, Friedman SL, Anania FA: Leptin in hepatic fibrosis: evidence for increased collagen production in stellate cells and lean littermates of ob/ob mice. Hepatology 2002, 35:762–771
4. Saxena NK, Titus MA, Ding X, Floyd J, Srinivasan S, Sitaraman SV, Anania FA: Leptin as a novel profibrogenic cytokine in hepatic stellate cells: mitogenesis and inhibition of apoptosis mediated by extracellular regulated kinase (Erk) and Akt phosphorylation. FASEB J 2004, 18:1612–1614
5. Angulo P: Nonalcoholic fatty liver disease. N Engl J Med 2002, 346:1221–1231
6. Chitturi S, Farrell GC: Etiopathogenesis of non-alcoholic steatohepatitis. Semin Liver Dis 2001, 21:27–41
7. Badger DA, Sauer JM, Hoglen NC, Jolley CS, Sipes IG: The role of inflammatory cells and cytochrome P450 in the potentiation of CCl4-induced liver injury by a single dose of retinol. Toxicol Appl Pharmacol 1996, 141:507–519
8. Hube F, Lietz U, Igel M, Jensen PB, Tornqvist H, Joost HG, Hauner H: Difference in leptin mRNA levels between omental and subcutaneous abdominal adipose tissue from obese humans. Horm Metab Res 1996, 28:690–693
9. Potter JJ, Womack L, Mezey E, Anania FA: Transdifferentiation of rat hepatic stellate cells results in leptin expression. Biochem Biophys Res Commun 1998, 244:178–182
10. Ikejima K, Takei Y, Honda H, Hirose M, Yoshikawa M, Zhang YJ, Lang T, Fukuda T, Yamashina S, Kitamura T, Sato N: Leptin receptor-mediated signaling regulates hepatic fibrogenesis and remodeling of extracellular matrix in the rat. Gastroenterology 2002, 122:1399–1410
11. Fitz JG, Basavappa S, McGill J, Melhus O, Cohn JA: Regulation of membrane chloride currents in rat bile duct epithelial cells. J Clin Invest 1993, 9:319–328
12. Truett GE, Bahary N, Friedman JM, Leibel RL: Rat obesity gene fatty (fa) maps to chromosome 5: evidence for homology with the mouse gene diabetes (db). Proc Natl Acad Sci USA 1991, 88:7806–7809
13. Chua SC, Chung WK, Wu-Peng XS, Zhang Y, Liu SM, Tartaglia L, Leiberl RL: Phenotypes of mouse diabetes and rat fatty due to mutations in the OB (leptin) receptor. Science 1996, 271:994–996
14. Chua SC, White DW, Wu-Peng XS, Liu SM, Okada N, Kershaw EE, Chung WK, Power-Kehoe L, Chua M, Tartaglia LA, Leibel RL: Phenotype of fatty due to Gln269Pro mutation in the leptin receptor (Lepr). Diabetes 1996, 45:1141–1143
15. Phillips MS, Liu Q, Hammond HA, Dugan V, Hey PJ, Caskey CJ, Hess JF: Leptin receptor missense mutation in the fatty Zucker rat. Nat Genet 1996, 13:18–19
16. Chitturi S, Farrell G, Frost L, Kriketos A, Lin R, Fung C, Liddle C, Samarasinghe D, George J: Serum leptin in NASH correlates with hepatic steatosis but not fibrosis: a manifestation of lipotoxicity? Hepatology 2002, 36:403–409
17. McCullough AJ, Bugianesi E, Marchesini G, Kalhan SC: Gender-dependent alterations in serum leptin in alcoholic cirrhosis. Gastroenterology 1988, 115:947–953
18. Sonnenberg GE, Krakower GR, Kissebah AH: A novel pathway to the manifestations of metabolic syndrome. Obes Res 2004, 12:180–186
19. Clark JM, Brancati FL, Diehl AM: The prevalence and etiology of elevated aminotransferase levels in the United States. Am J Gastroenterol 2003, 98:960–967
20. Xu A, Wang Y, Keshaw H, Xu LY, Lam KSL, Cooper GJS: The fat-derived hormone adiponectin alleviates alcoholic and nonalcoholic fatty liver diseases in mice. J Clin Invest 2003, 112:91–100
21. Kamada Y, Tamura S, Kiso S, Matsumoto H, Saji Y, Yoshida Y, Fukui K, Maeda N, Nishizawa H, Nagaretani H, Okamoto Y, Kihara S, Miyagawa J, Shinomura Y, Funahashi T, Matsuzawa Y: Enhanced carbon tetrachloride-induced liver fibrosis in mice lacking adiponectin. Gastroenterology 2003, 125:1796–1807
22. Pittas AG, Joseph NA, Greenberg AS: Adipocytokines and insulin resistance. J Clin Endocrinol Metab 2004, 89:447–452
23. Tsao TS, Lodish HF, Fruebis J: ACRP30, a new hormone controlling fat and glucose metabolism. Eur J Pharmacol 2002, 440:213–221
24. Fruebis J, Tsao TS, Javorschi S, Ebbets-Reed D, Erickson MR, Yen FT, Bihain BE, Lodish HF: Proteolytic cleavage product of 30-kDa adipocyte complement-related protein increases fatty acid oxidation in muscle and causes weight loss in mice. Proc Natl Acad Sci USA 2001, 98:2005–2010
25. Yamauchi T, Kamon J, Ito Y, Tsuchida A, Yokomizo T, Kita S, Sugiyama T, Miyagishi M, Hara K, Tsunoda M, Murakami K, Ohteki T, Uchida S, Takekawa S, Waki H, Tsuno NH, Shibata Y, Terauchi Y, Froguel P, Tobe K, Koyasu S, Taira K, Kitamura T, Shimizu T, Nagai R, Kadowaki T: Cloning of adiponectin receptors that mediate antidiabetic metabolic effects. Nature 2003, 423:762–769
26. Yamauchi T, Kamon J, Minokoshi Y, Ito Y, Waki H, Uchida S, Yamashita S, Noda M, Kita S, Ueki K, Eto K, Akanuma Y, Froguel P, Foufelle F, Ferre P, Carling D, Kimura S, Nagai R, Kahn BB, Kadowaki T: Adiponectin stimulates glucose utilization and fatty-acid oxidation by activating AMP-activated protein kinase. Nat Med 2002, 8:1288–1295
27. Tomas E, Tsao TS, Saha AK, Murrey HE, Zhang CC, Itani SI, Lodish HF, Ruderman NB: Enhanced muscle fat oxidation and glucose transport by ACRP30 globular domain: acetyl-CoA carboxylase inhibition and AMP-activated protein kinase activation. Proc Natl Acad Sci USA 2002, 99:16309–16313
28. Te Sligte K, Bourass I, Sels JP, Driessen A, Stockbrugger RW, Koek GH: Non-alcoholic steatohepatitis: review of a growing medical problem. Eur J Intern Med 2004, 15:10–21
29. Wang Y, Xu A, Knight C, Xu LY, Cooper GJS: Hydroxylation and glycosylation of the four conserved lysine residues in the collagenous domain of adiponectin. J Biol Chem 2002, 77:19521–19529
30. Kurosawa H, Que FG, Roberts LR, Fesmier PJ, Gores GJ: Hepatocytes in the bile duct-ligated rat express Bcl-2. Am J Physiol 1997, 272:G1587–G1593
31. Janqueira L, Bignolas G, Bretani R: Picrosirius staining plus polarization microscopy: a specific method for collagen detection in tissue sections. Histochem J 1979, 11:447–455
32. Rasmussen RP: Quantification on the LightCycler. Rapid Cycle Real Time PCR. Edited by Meuer S, Witwer CT, Nakagawata K. New York, Springer, 2000, pp 21–34
33. Rire KM, Rasmussen RP, Wittwer CT: Product differentiation by analysis of DNA melting curves during the polymerase chain reaction. Anal Biochem 1997, 245:154–160

34. Wilhelm J, Pingoud A: Real-time polymerase chain reaction. Chembiochem 2003, 4:1120–1128
35. Friedman SL, Roll FJ: Isolation and culture of hepatic lipocytes, Kupffer cells, and sinusoidal endothelial cells by density gradient centrifugation with Stractan. Anal Biochem 1987, 161:207–218
36. Bradford MM: A rapid and sensitive method for the quantitation of microgram quantities of protein utilizing the principle of protein-dye binding. Anal Biochem 1976, 72:248–254
37. Laemmli UK: Cleavage of structural proteins during the assembly of the head of bacteriophage T4. Nature 1970, 227:680–685
38. Dudek H, Datta SR, Franke TF, Birnbaum RY, Cooper GM, Segal RA, Kaplan DR, Greengerg ME: Regulation of neural survival by the serine-threonine protein kinase Akt. Science 1997, 275:661–665
39. Han YP, Zhou L, Wang J, Xiong S, Garner WL, French SW, Tsukamoto H: Essential role of matrix metalloproteinases in interlukin-1-induced myofibroblastic activation of hepatic stellate cell in collagen. J Biol Chem 2004, 279:48520–48528
40. Yang SQ, Lin HZ, Lane MD, Clemens M, Diehl AM: Obesity increases sensitivity to endotoxin liver injury: implications for the pathogenesis of steatohepatitis. Proc Natl Acad Sci USA 1997, 94:2557–2562
41. Koteish A, Diehl AM: Animal models of steatosis. Semin Liver Dis 2001, 21:89–104
42. Schnur J, Olah J, Szepesi A, Nagy P, Thorgeirsson SS: Thioacetamide-induced hepatic fibrosis in transforming growth factor beta-1 transgenic mice. Eur J Gastroenterol Hepatol 2004, 16:127–133
43. Hotta K, Funahashi T, Bodkin NL, Ortmeyer HK, Arita Y, Hansen BC, Matsuzawa Y: Circulating concentrations of the adipocyte protein adiponectin are decreased in parallel with reduced insulin sensitivity during the progression to type 2 diabetes in rhesus monkeys. Diabetes 2001, 50:1126–1133
44. Ouchi N, Kihara S, Arita Y, Nishida M, Matsuyama A, Okamoto Y, Ishigami M, Kuriyama H, Kishida K, Nishizawa H, Hotta K, Muraguchi M, Ohmoto Y, Yamashita S, Funahashi T, Matsuzawa Y: Adipocyte-derived plasma protein, adiponectin, suppresses lipid accumulation and class A scavenger receptor expression in human monocyte-derived macrophages. Circulation 2001, 103:1057–1063
45. Kumada M, Kihara S, Sumitsuji S, Kawamoto T, Matsumoto S, Ouchi N, Arita Y, Okamoto Y, Shimomura I, Hiraoka H, Nakamura T, Funahashi T, Matsuzawa Y, the Osaka CAD Study Group: Association of hypoadiponectinemia with coronary artery disease in men. Arterioscler Thromb Vasc Biol 2003, 23:85–89
46. Brakenhielm E, Veitonmaki N, Cao R, Kihara S, Matsuzawa Y, Zhivotovsky B, Funahashi T, Cao Y: Adiponectin-induced antiangiogenesis and antitumor activity involve caspase-mediated endothelial cell apoptosis. Proc Natl Acad Sci USA 2004, 101:2476–2481
47. Montague CT, Prins JB, Sanders L, Zhang J, Sewter CP, Digby J, Byrne CD, O'Rahilly S: Depot-related gene expression in human subcutaneous and omental adipocytes. Diabetes 1998, 47: 1384–1391
48. Fasshauer M, Paschke R: Regulation of adipocytokines and insulin resistance. Diabetologia 2003, 46:1594–1603
49. Liefers SC, te Pas MF, Veerkamp RF, Chilliard Y, Delavaud C, Gerritsen R, van der Lende T: Association of leptin gene polymorphisms with serum leptin concentration in dairy cows. Mamm Genome 2003, 14:657–663
50. Han DC, Isono M, Chen S, Casaretto A, Hong SW, Wolf G, Ziyadeh FN: Leptin stimulates type I collagen production in db/db mesangial cells: glucose uptake and TGF-beta type II receptor expression. Kidney Int 2001, 9:1315–1323
51. Guerre-Millo M: Adipose tissue and adipokines: for better or worse. Diabetes Metab 2004, 30:13–19
52. Fruebis J, Tsao TS, Javorschi S, Ebbets-Reed D, Erickson MR, Yen FT, Bihain BE, Lodish HF: Proteolytic cleavage product of 30-kDa adipocytes complement-related protein increases fatty acid oxidation in muscle and causes weight loss in mice. Proc Natl Acad Sci USA 2001, 98:2005–2010
53. Yamauchi T, Kamon J, Minokoshi Y, Ito Y, Waki H, Uchida S, Yamashita S, Noda M, Kita S, Ueki K, Eto K, Akanuma Y, Froguel P, Foufelle F, Ferre P, Carling D, Kimura S, Nagai R, Kahn BB, Kadowaki T: Adiponectin stimulates glucose utilization and fatty-acid oxidation by activating AMP-activated protein kinase. Nat Med 2002, 8:1288–1295
54. Tomas E, Tsao TS, Saha AK, Murrey HE, Zhang CC, Itani SI, Lodish HF, Ruderman NB: Enhanced muscle fat oxidation and glucose transport by ACRP30 globular domain: acetyl-CoA carboxylase inhibition and AMP-activated protein kinase activation. Proc Natl Acad Sci USA 2002, 99:16309–16313
55. Yamauchi T, Kamon J, Waki H, Imai Y, Shimozawa N, Hioki K, Uchida S, Ito Y, Takakuwa K, Matsui J, Takata M, Eto K, Terauchi Y, Komeda K, Tsunoda M, Murakami K, Ohnishi Y, Naitoh T, Yamamura K, Ueyama Y, Froguel P, Kimura S, Nagai R, Kadowaki T: Globular adiponectin protected ob/ob mice from diabetes and ApoE-deficient mice from atherosclerosis. J Biol Chem 2003, 278:2461–2468